



A STUDY OF THE INTERFACIAL HEAT TRANSFER COEFFICIENT IN POROUS BURNERS

Roberto Carlos Moro Filho

Escola de Ciências e Tecnologia
Universidade Federal do Rio Grande do Norte
Caixa Postal 1524, Campus Universitário Lagoa Nova
59072-970 – Natal – RN - Brasil
moro@ect.ufrn.br

Abstract. *The present work investigate the couple between the solid energy equation and the fluid energy equation in a porous radiant burner. The volumetric heat transfer coefficient is the responsible by the couple between the two energy equations, related to the solid phase and the fluid phase, and it has been a source of great uncertainty in the literature. Traditionally, the literature presents the determination of the effective properties of just simple geometries through analytical results, numerical simulations and experimental approach. Recently a new approach has been presented in the literature, consisting in the determination of the effective transport properties by tomography-based direct pore level numerical simulation (DPLS). In the present work the correlation obtained by the DPLS is compared with the correlations obtained by another methods and the effect in the pollutant emissions is presented. A laminar two dimensional model is based on a macroscopic formulation of the transport equations. A 6 step reduced mechanism is adopted to model the chemical kinetics and a finite volume method is used for the simulation.*

Keywords: *numerical simulation, combustion, porous burner.*

1. INTRODUCTION

Reactive flow in porous media occurs in a wide range of processes. Systems based on fluidized bed combustion, ground water pollution, catalytic reactors, metallurgy, cement production, exhaust gas treatment, fuel processing, in-situ combustion for oil recovery, household heating combustion, are a few examples of such applications. Analysis of the transport phenomena in porous media and the complex interactions between the fluid phase and the solid phase is fundamental to understand these processes.

Studies on macroscopic transport modeling of incompressible flows in porous media have been based on the volume-average methodology (continuum models) for either heat or mass transfer. The accuracy of continuum models relies on the effective transport properties adopted in the calculations. The determination of the effective transport parameters suffers from several drawbacks. The analysis of transport phenomena in reticulate porous ceramic (RPC) is complex, some of the pores are open, some are closed and some are partly open and partly closed. Even samples of the same manufacturer show differences in the mean pore diameter. The geometry, shape and size distribution of the pores varies with the method of manufacturing.

Basically, there are two common (traditional) methods to determine effective properties. One method involves the numerical simulations of the flow and heat transfer at a pore level utilizing a simple geometry to represent the real porous medium (Kuwahara *et al.*, 2001). Another usual method consists of applying an experimental technique in conjunction with an inverse analysis (Fu *et al.*, 1998).

Recently, with the advent of high performance computers and the improvement in obtain good geometrical representation of the porous medium by high resolution computer tomography, a third method can be employed. It consists in the tomography-based direct pore level numerical simulation (DPLS), which is a general method for the determination of effective transport properties. This method is putting in check some of the classical methods for porous media. Within the limits of the numerical truncation error and the accuracy of the geometrical representation related to the statistical treatment, DPLS approaches the exact solution (Petrasch *et al.*, 2007).

The author of the present article has been investigating the effective properties of RPCs through the numerical simulations of radiant porous burners. The sensitivity analyses of the effective thermal conductivity and the Rosseland mean attenuation coefficient were presented by Moro and Pimenta (2011). The correlations to the Nusselt Number obtained by the traditional methods and the effect on the temperature field were presented in Moro and Pimenta (2009).

The purpose of the present work is to investigate the outcome of the choice of the correlation adoption to the Nusselt number on the temperature field and on the CO emissions. The correlations to the Nusselt number available in the literature obtained by the traditional methods (Fu *et al.*, 1998; Kuwahara *et al.*, 2001) and the correlation obtained by the DPLS (Petrasch *et al.*, 2007), considered more accurate, are tested. The comparison of the numerical results utilizing the different correlations, provide important information about the errors that the use of the traditional correlations result.

2. MACROSCOPIC TRANSPORT EQUATIONS

2.1. Macroscopic continuity equation

$$\phi \frac{\partial \rho}{\partial t} + \nabla \cdot (\rho \mathbf{u}_D) = 0 \quad (1)$$

where, \mathbf{u}_D is the average surface velocity (also known as seepage, superficial, filter or Darcy velocity). Equation (1) represents the macroscopic continuity equation for an incompressible fluid.

2.2. Macroscopic momentum equation

The heuristic macroscopic momentum equation utilized in this work is found in the literature (Kaviany, 1995; Pedras, 2000) and corresponds to an attempt of the scientific community to develop an equation, based on a volume-averaged treatment of the flow field, along the lines of Navier-Stokes equation. Another desirable characteristic of this heuristic equation is that it can describe both the momentum transport through the porous media as well as that in the plain media.

$$\frac{\partial (\rho \mathbf{u}_D)}{\partial t} + \nabla \cdot \left(\frac{\rho \mathbf{u}_D \mathbf{u}_D}{\phi} \right) = -\nabla (\phi p) + \mu \nabla^2 \mathbf{u}_D - \left[\frac{\mu \phi}{K} \mathbf{u}_D + \frac{c_F \phi \rho |\mathbf{u}_D| \mathbf{u}_D}{\sqrt{K}} \right] \quad (2)$$

where the last two terms in Eq. 2, represent the Darcy-Forchheimer contribution (Pedras, 2000). The symbol K is the porous medium permeability, $c_F = 0.55$ is the form drag coefficient (Forchheimer coefficient), p is the intrinsic (volume-averaged on fluid phase) pressure of the fluid, ρ is the fluid density and is a function of temperature, μ represents the fluid dynamic viscosity and ϕ is the porosity of the porous medium.

2.3. Macroscopic Two-Energy Equations Model

In this work the effects of dispersion and tortuosity are neglected.

$$\left\{ (\rho c_p)_f \phi \right\} \frac{\partial T_f}{\partial t} + (\rho c_p)_f \nabla \cdot (\mathbf{u}_D T_f) = \nabla \cdot \left\{ \mathbf{K}_{eff,f} \cdot \nabla T_f \right\} + h_v (T_s - T_f) + \phi \sum_{k=1}^{Nsp} w_k M_k h_k \quad (3)$$

and

$$\left\{ (1-\phi)(\rho c_p)_s \right\} \frac{\partial T_s}{\partial t} = \nabla \cdot \left\{ \mathbf{K}_{eff,s} \cdot \nabla T_s \right\} - h_v (T_s - T_f) \quad (4)$$

represent the energy equation for fluid and solid phase, respectively, where, T_f and T_s are the intrinsic volume average of the temperatures of the fluid phase and solid phase (Kaviany, 1995; Saito, 2006), h_v is the volumetric heat transfer coefficient and $\mathbf{K}_{eff,f}$ and $\mathbf{K}_{eff,s}$ are the effective conductivity tensors for the fluid and the solid phase, respectively, given by:

$$\mathbf{K}_{eff,f} = \left[\phi k_f \right] \mathbf{I} \quad (5)$$

$$\mathbf{K}_{eff,s} = (1-\phi) \left[k_s + \frac{16\sigma \langle T_s \rangle^3}{3K_r} \right] \mathbf{I} \quad (6)$$

where, k_f and k_s are the thermal conductivities for the fluid and for the solid, respectively, K_r is the local Rosseland mean attenuation coefficient, σ is the Stefan-Boltzmann constant. The radiation in an optically dense medium can be

modeled using the diffusion approximation or Rosseland model (Siegel and Howell, 2002). In the radiative diffusion approximation the radiation is computed like an increase in the effective conductivity and is represented by the term containing K_r in Eq. 6.

The energy equations of the solid and fluid phases are coupled through the convection term and in this term there is the volumetric heat transfer coefficient (h_v). There are in the literature many empirical correlations that can be used to calculate the h_v . These correlations involves the Nusselt number and the Reynolds number. The choice of a characteristic length for correlating heat transfer data in terms of Nusselt and Reynolds numbers represent an important technical issue. Lengths based on average particle diameter (d_p), mean pore diameter (d_m), the square root of permeability ($K^{1/2}$), the hydraulic diameter (d_h) and others are found in the correlations presented in the literature. The relation between the h_v , that has the dimensions $W/m^3 \cdot K$, and the conventional convective heat transfer coefficient h , that has the dimensions $W/m^2 \cdot K$, is $h_v = a_v h$, where a_v is the specific surface area (i.e., area per unit volume). In the literature some authors present correlations involving h and others, h_v .

Fu *et al.* (1998) determined experimentally, through one inverse method, the h_v of five different ceramics with different porosities and a wide range of Reynolds numbers. The authors developed an empirical correlation to the volumetric Nusselt number:

$$Nu_v = \frac{h_v d_m^2}{k_f} = C Re^m \quad (7)$$

Kuwahara *et al.* (2001) present a numerical procedure, purely theoretical. Considered the flow through square rods placed in a staggered fashion. The square rods were maintained at a constant temperature. The Reynolds was varied from 10^{-2} to 10^3 and the porosity from 0.36 to 0.96, whereas the Prandtl number was varied from 10^{-2} to 10^2 . From the numerical experiments, Kuwahara *et al.* (2001) provided the following expression:

$$Nu = \frac{hD}{k_f} = \left(1 + \frac{4(1-\phi)}{\phi}\right) + \frac{1}{2}(1-\phi)^{1/2} Re_D^{0.6} Pr^{1/3}, \text{ where, } 0.2 < \phi < 0.9 \quad (8)$$

Petrasch *et al.* (2008) presented a modern technique consisting in generating a 3D pore-level digital representation through the high resolution computer tomography images and then apply the direct pore level numerical simulation (DPLS) of the fluid flow and heat transfer to determine the effective properties. Petrasch *et al.* (2008) obtained the following expression to the mean Nusselt number:

$$Nu = d_0 + d_1 \cdot Re^{d_2} Pr^{d_3} \quad (9)$$

where, $d_0=1.5590$, $d_1=0.5954$, $d_2=0.5626$ and $d_3=0.4720$.

2.4. Macroscopic Mass Transport Equation

$$\frac{\partial(\rho \phi y_k)}{\partial t} + \nabla \cdot (\rho \mathbf{u}_D y_k) = \nabla \cdot [\rho \mathbf{D}_{eff} \cdot \nabla(\phi y_k)] + \phi w_k \dot{M}_k \quad (10)$$

where y_k is the local mass fraction for the species k. The effective dispersion tensor D_{eff} is defined as:

$$\mathbf{D}_{eff} = \mathbf{D}_{disp} + \mathbf{D}_{diff} = \mathbf{D}_{disp} + \frac{1}{\rho} \left(\frac{\mu}{Sc} \right) \mathbf{I} \quad (11)$$

where, Sc is the Schimidt number, D_{diff} is the macroscopic diffusion tensor, and D_{disp} is the mass dispersion tensor (Mesquita, 2003). The effects of dispersion are neglected in this work, therefore, the effective dispersion tensor is given by:

$$\mathbf{D}_{eff} = \frac{1}{\rho} \left(\frac{\mu}{Sc} \right) \mathbf{I} \quad (12)$$

2.5. Boundary conditions

The figure 1 presents the boundary conditions to the cylindrical porous burner, where: q_s is the heat flux at the exit, q_r the heat flux due to the radiation and q_w the heat flux at the wall of the burner. The surface of the packed bed radiates energy to the surrounding surfaces according to the equation below:

$$q_r = -K_{eff} \frac{\partial T}{\partial x} = (\varepsilon_{eff} \sigma T^4 - \alpha_{eff} \sigma T_{\infty}^4) \quad (13)$$

where, ε_{eff} is effective emissivity, α_{eff} is the effective absorptivity of the porous bed and T_{∞} is the ambient temperature. The ε_{eff} and α_{eff} are equal to simplify the solution.

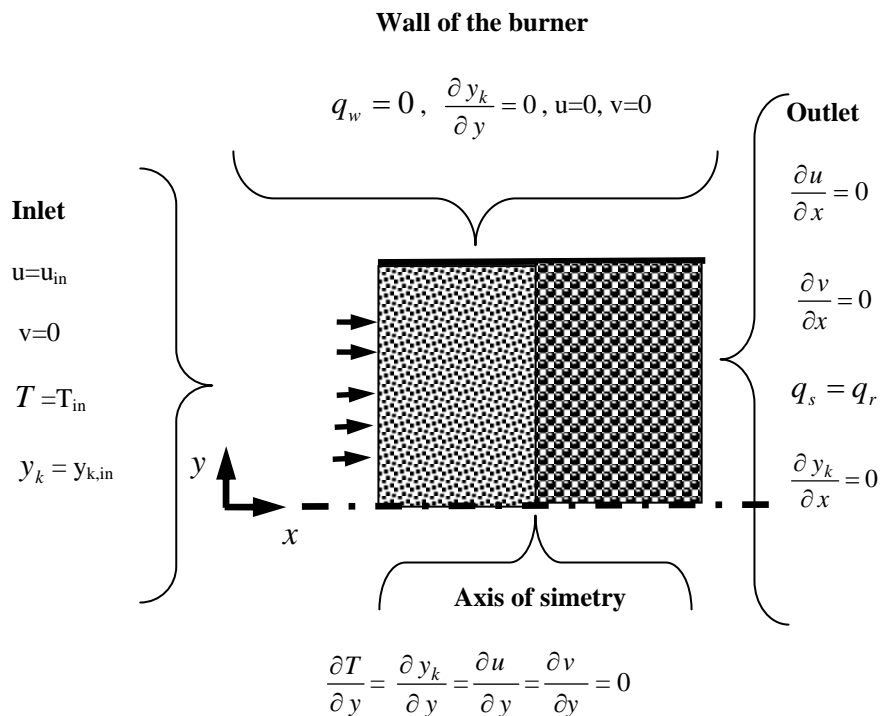


Figure 1. Boundary conditions

2.6. Combustion model

The method to solve the chemical kinetic problem utilizes two models to describe the reaction process, a global reaction mechanism and a six step reaction mechanism.

2.6.1. One-step global mechanism

The combustion reaction is assumed to occur in a single step according to the chemical equation



where, ψ is the excess air in the reactant stream at the inlet of porous foam and is related to the equivalence ratio Φ by,

$$\Psi = \frac{1}{\Phi} - 1 \quad (15)$$

where,

$$\Phi = \frac{(y_{fu} / y_{ox})}{(y_{fu} / y_{ox})_{st}} \quad (16)$$

The ratio of fuel consumption is given by,

$$S_{fu} = \rho^2 A y_{fu} y_{ox} \exp(-E_a / RT) \quad (17)$$

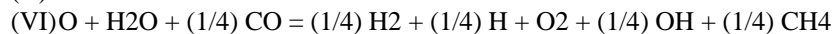
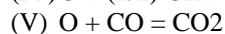
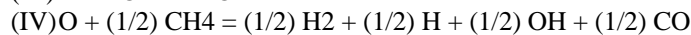
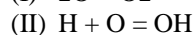
where, A is the pre-exponential factor, Ea is the activation energy and R is the universal gas constant. The gas density is updated using the ideal gas equation in the form,

$$\rho = P_0 / R^* T \quad (18)$$

where, P₀ is a reference pressure, which is kept constant during the relaxation process, and $R^* = R / M$ and M is the gas molecular mass.

2.6.2. Six-step reduced mechanism

Chang and Chen have developed a six-step reduced mechanism with an automatic computer code (CARM) from GRI-MECH 1.2:



3. NUMERICAL MODEL

The governing equations were discretized using the finite volume procedure (Patankar, 1980) with a boundary-fitted non-orthogonal coordinate system. The system of algebraic equations was solved through the semi-implicit procedure according to Stone (1968). The SIMPLE algorithm for the pressure-velocity coupling was adopted to correct both the pressure and the velocity fields. The process starts with the solution of the two momentum equations. Then the velocity field is adjusted in order to satisfy the continuity principle. This adjustment is obtained by solving the pressure correction equation. To simulate the combustion utilizing the Six-step reduced mechanism the energy and species equations are solved using a fractional time step method (Yanenko, 1971) to eliminate the problems arising from the stiffness of the system. It was adopted the minimum residence time of the gas in all control volumes as the integration time step. Calculations start using one-step global kinetics mechanism, when the residuals reach 1×10^{-3} the multistep mechanism is switched on and the fractional time step method is applied (Malico *et al.*, 2000). A computational mesh of 266×34 is adopted in the simulations.

All computations were performed on an Intel(R) Xeon(R) 3.40 GHz, 16GB. For all cases a relative convergence of 10^{-5} was specified. The grid effects on the solutions were examined by increasing the number of nodes and verifying the solutions until the results no longer changed in a specified tolerance.

4. RESULTS AND DISCUSSION

The parameters for the one-step global mechanism are the same to all cases. The activation energy, Ea, and the pre-exponential factor, A, were taken from Mohamad *et al.* (1994) and are 140×10^3 J/mol and 1×10^{10} m³kg⁻¹s⁻¹, respectively.

4.1. Burner simulated

Figure 2 presents a two-dimensional axisymmetric geometry corresponding to the porous media burner developed and tested at UFSC-Universidade Federal de Santa Catarina (Pereira, 2002). The reactor consists of two distinct regions

with different porosities and permeabilities, the gas mixture enters at the inflow boundary on the left (preheating region), and the combustion products leave the burner at the outflow boundary on the right (combustion region). In the preheating region a mixture of 65% of zirconium oxide (ZrO_2) and 35% of alumina (Al_2O_3) was utilized, 15.74 pores per centimeter (ppcm), and 86% of porosity. In the combustion region the same material of the preheating region was utilized, with 3.9 ppcm, and 90% of porosity. The walls are impermeable and isolated with a mix of alumina (Al_2O_3). The numerical parameters are found in table 1.

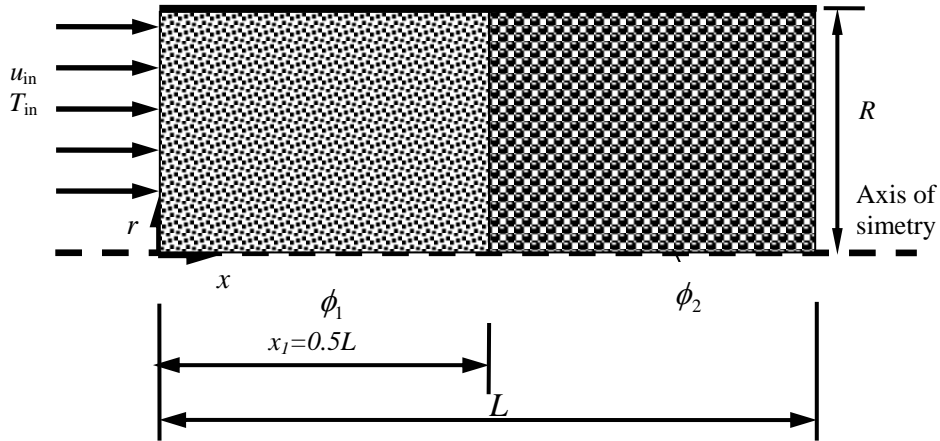


Figure 2. Geometry of a cylindrical porous burner and coordinate system

4.2. Temperature and CO mass fraction profiles with different h_v correlations

The volumetric heat transfer coefficient (h_v), which is in the convective term, is responsible by the couple between the two energy equations and it is a source of great uncertainty in the literature. Many researchers investigated h_v in experiments involving or not combustion.

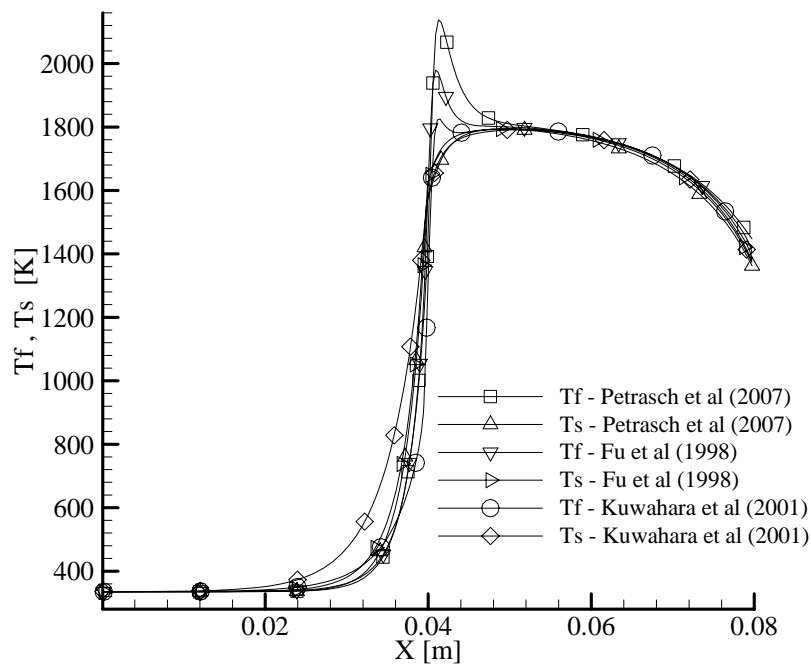


Figure 3: Fluid and solid temperatures profiles at the center line ($r=0$) obtained utilizing different correlations to h_v : Kuwahara *et al.* (2001), Fu *et al.* (1998) and DPLS presented by Petrasch *et al.* (2007)

The Fig. 3 presents the solid and fluid temperature profiles in the center line of the reactor utilizing a global one-step global mechanism. The temperatures of the solid and the fluid phase were obtained employing three different correlations to the Nusselt number. The correlations presented by Petrasch *et al.* (2007) and by Fu *et al.* (1998) considered the mean pore diameter as the characteristic length. The correlation presented by Kuwahara *et al.* (2001) considered the particle diameter (d_p) as the characteristic length. The porosity (ϕ), specific surface area (a_v) and mean pore diameter (d_m) are the parameters considered to characterize the geometric structure of the porous materials utilized in the reactor. The values adopted in the simulations can be found in Tab 1. To test the correlation presented by Kuwahara *et al.* (2001) in order to compare with the results calculated utilizing the correlation proposed by Petrasch *et al.* (2007) and by Fu *et al.* (1998), it is necessary to consider the porosity and the specific area provided by Petrasch *et al.* (2007) and by Fu *et al.* (1998) and to calculate the particle diameters through the following expression:

$$d_p = \frac{4(1-\phi)}{a_v} \quad (19)$$

In spite of the DPLS method is considered very accurate, the sample utilized by Petrasch *et al.* (2007) doesn't correspond to that considered by Pereira (2002). The values of the pore diameter adopted in these simulations, probably, do not correspond to the real mean values. The mean pore diameters are estimated through the values of the number of pores per centimeter (PPC) provided by Pereira (2002). The peak temperature of the fluid phase in the DPLS profile presented in Fig. 3 is too high. The peak temperature of the fluid phase has a strong dependence on the mean pore diameter as can be seen in the Fig. 4, where is presented a simulation with just one porous matrix and three different mean pore diameters. Probably, the real mean pore diameter of the region 2 of the reactor, is smaller than the value calculated making use of PPC values provided by Pereira (2002). To the same porosity, as smaller the value of the pore diameter, higher it is the specific area and the heat transfer between the two phases.

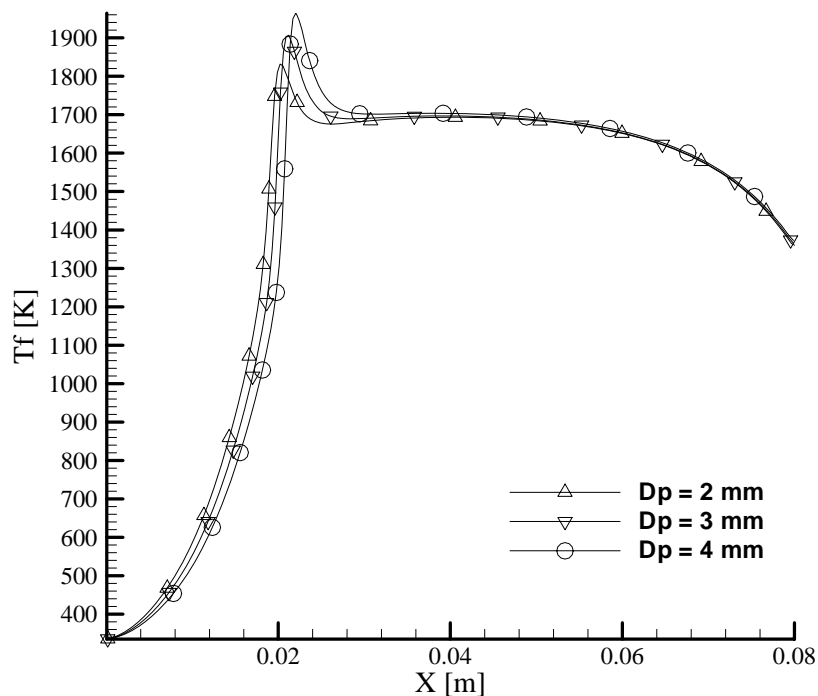


Figure 4: Fluid temperature profiles at the center line ($r=0$) of a porous burner with just one material ($\phi = 0.86$), obtained utilizing different values of the mean pore diameter (D_p)

The peak temperature of the fluid phase obtained with the correlation presented by Fu *et al.* (1998) is 7.3% lower than that obtained making use of the correlation developed by Petrasch *et al.* (2007). The peak temperature of the fluid phase obtained with the correlation presented by Kuwahara *et al.* (2001) is 14.6% smaller than that obtained with the correlation presented by Petrasch *et al.* (2007). The results obtained employing the correlation provided by Kuwahara *et al.* (2001), represent a situation closer of thermal equilibrium between the solid and fluid phases.

The Fig. 5 presents the fluid temperature obtained with different Nusselt correlations and with the six-step reaction mechanism. No peaks appear in the fluid temperature curves when utilizing the six-step reaction mechanism.

R.C. Moro Filho
A Study of the Interfacial Heat Transfer Coefficient in Porous Burners

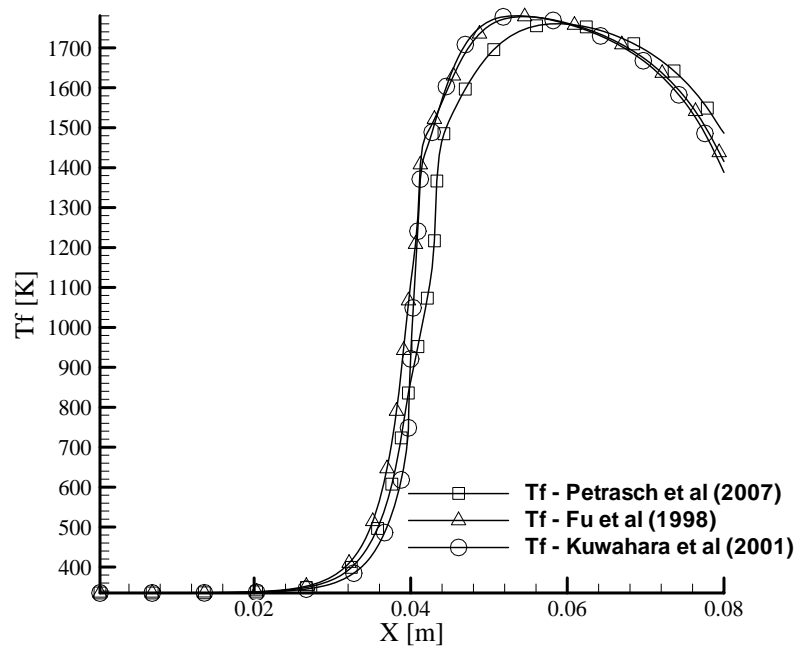


Figure 5: Fluid temperatures profiles at the center line ($r=0$) obtained utilizing different correlations to h_v : Kuwahara *et al.* (2001), Fu *et al.* (1998) and DPLS presented by Petrasch *et al.* (2007);

The Fig. 6 presents the CO mass fraction profiles obtained with different Nusselt correlations and with the six-step reaction mechanism. The results of the simulations using the correlation obtained by Petrasch *et al.* (2007) are compared with the results obtained by the use of the correlations presented by Fu *et al.* (1998) and Kuwahara *et al.* (2001). The mean CO mass fraction at the exit of the reactor obtained with the correlation presented by Fu *et al.* (1998) is 12.9% lower than that obtained making use of the correlation developed by Petrasch *et al.* (2007). The mean CO mass fraction obtained using the Kuwahara *et al.* (2001) correlation was 16.4% smaller than that obtained with the correlation found by Petrasch *et al.* (2007).

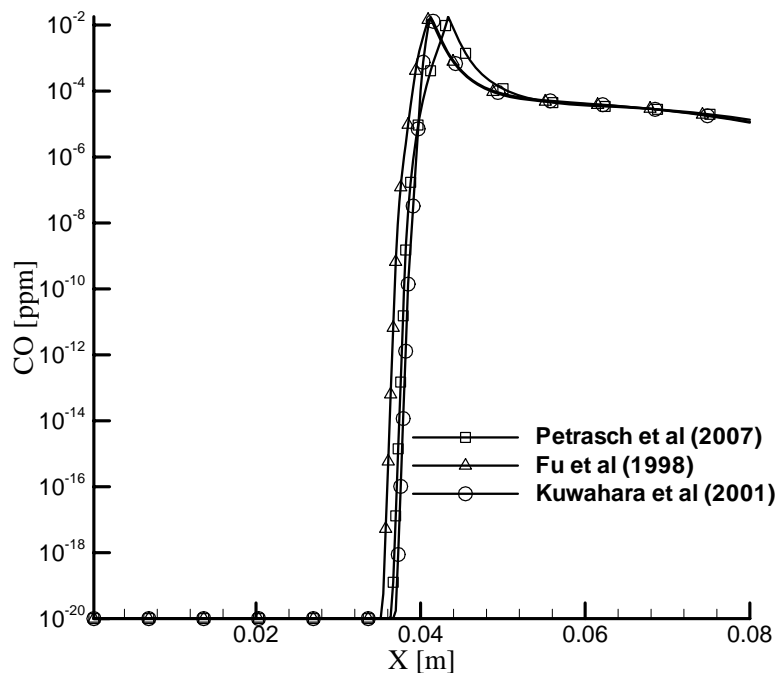


Figure 6: CO mass fraction profiles at the center line ($r=0$) obtained utilizing different correlations to h_v : Kuwahara *et al.* (2001), Fu *et al.* (1998) and DPLS presented by Petrasch *et al.* (2007);

5. CONCLUSION

The Nusselt correlations obtained by an experimental technique (Fu et al., 1998), by DPLS (Petrasch et al., 2007) and by numerical simulation considering a simple geometry (Kuwahara et al., 2001) were tested and the results of temperature and CO profiles compared. In spite of the simplicity of the geometry adopted by Kuwahara et al. (2001), square rods placed in a staggered fashion, the results of the CO emissions are reasonable. The values of the mean pore diameters calculated through the PPC provided by the manufacturer do not correspond to real mean values. It would be necessary to obtain the values of the mean pore diameter and the specific area of these materials utilized in the reactor through the DPLS method to run simulations that provide accurate results. The results obtained with the one-step global mechanism present peaks of temperature in the fluid phase. The results with the six-step reaction mechanism do not present peaks of temperature in the fluid phase. There are several characteristic times involved in the chemical reactions and transport mechanisms of heat and mass. The characteristic times involved in the combustion can not be presented through a global model. On the other hand, the methodology employed to solve the problem considering 10 species provides an enormous amount of parameters to be checked.

6. ACKNOWLEDGEMENTS

The author is thankful to Federal University of Rio Grande do Norte (UFRN), Brazil, for their financial support during the preparation of this work.

Table 1. Operating Conditions

Quantity	Value
Activation energy (J/mol) - Ea	1.4×10^8
Pre-exponential factor in reaction rate – A (m ³ /kg.s)	1×10^{10}
Length of the combustor – L (cm)	8
D (cm)	4
R (kJ/kmol.K)	8.3145
R* (kJ/kgK)	0.301
P ₀ (kN/m ²)	101.325
y _{fuel,in}	0.033784
T _{in} (K)	335
Matrix 1:	
K ₁ (m ²)	1.477×10^{-8}
ϕ_1	0.86
a _{v1}	1060 m ⁻¹
Matrix 2:	
K ₂ (m ²)	3.698×10^{-7}
ϕ_2	0.90
a _{v2}	960 m ⁻¹

7. REFERENCES

- Chang, W.C., and Chen, J.Y., Reduced Mechanisms based on GRI-Mech 1.2, <http://firebrand.me.berkeley.edu/griredu.html>
- Fu, X., Viskanta, R., Gore, J.P., 1998, Measurement and correlation of volumetric heat transfer coefficients of cellular ceramics, *Experimental Thermal and Fluid Science*, Vol. 17, pp. 285-293.
- Kaviany. M.. 1995. Principles of Heat Transfer in Porous Media. 2nd edn. Springer. New York.
- Kee, R. J., Rupley, F. M., Miller, J. A., Coltrin, M. E., Grcar, J. F., Meeks, E., Moffat, H. K., Lutz, A. E., Dixon-Lewis, G., Smooke, M. D., Warnatz, J., Evans, G. H., Larson, R. S., Mitchell, R. E., Petzold, L. R., Reynolds, W. C., Caracotsios, M., Stewart, W. E., Glarborg, P., Wang, C., Adigun, O., Houf, W. G., Chou, C. P., and Miller, S. F., Thermodynamic data is part of the CHEMKIN Collection. Chemkin Collection, Release 3.7, Reaction Design, Inc., San Diego, CA (2002).

R.C. Moro Filho

A Study of the Interfacial Heat Transfer Coefficient in Porous Burners

- Kuwahara, F., Shiota, M., Nakayama, A., 2000, A numerical study of the interfacial convective heat transfer coefficient in two-energy equation model for convection in porous media, *International Journal of Heat and Mass Transfer*, Vol. 44, pp. 1153-1159.
- Malico, I., Zhou, X.Y., and Pereira, J.C.F., 2000, Two-dimensional Numerical Study of Combustion and Polutants Formation in Porous Burners, *Combust. Sci. and Tech.*, 152, pp. 57-79.
- Mesquita, M.S., 2003, Análise da dispersão mássica em meios porosos em regimes laminar e turbulento. Tese de doutorado, Instituto Tecnológico de Aeronautica, Brasil.
- Mohamad, A.A., Ramadhyani, S., Viskanta, R., 1994. Modeling of Combustion and Heat-Transfer in a Pcked-Bed with Embedded Coolant Tubes, *Int. J Heat and Mass Transfer*. vol. 37. (8) pp.1181-1191.
- Moro Filho, R. C.; Pimenta, A., 2011. A Two-Dimensional Numerical Simulation of Combustion and Heat Transfer in Radiant Porous Burners. *Combustion Science and Technology*. , v.183, p.370 - 389.
- Moro Filho, R. C.; Pimenta, Amilcar, 2009. A numerical study of combustion in porous burner with a two-energy equation model, Gramado-RS, 20th International Congress of Mechanical Engineering.
- Patankar. S. V., 1980. *Numerical Heat Transfer and Fluid Flow*. Hemisphere. New York.
- Pedras, M.H.J., 2000, Análise do Escoamento Turbulento em Meio Poroso Descontínuo. Tese de doutorado, Instituto Tecnológico de Aeronautica, Brasil.
- Pereira, F.M., 2002, Medição de características térmicas e estudo do mecanismo de estabilização de chama em queimadores porosos radiantes. Tese de Mestrado, Universidade Federal de Santa Catarina, Brasil.
- Petrasch, J., Meier, F., Friess, H., Steinfeld, A., 2007, Tomography based determination of permeability, Dupuit-Forchheimer coefficient, and interfacial heat transfer coefficient in reticulate porous ceramics, *International Journal of Heat and Fluid Flow*, Vol. 29, pp. 315-326.
- Saito, M. B., 2006, Analysis of Thermal Non-Equilibrium for Turbulent Transport in Porous Media, Tese de doutorado, Instituto Tecnológico de Aeronautica, Brasil.
- Sathe, S.B., Peck, R.E., and Tong, T.W., 1990, A numeriacal analysis of heat transfer and combustion in porous radiant burners, *Int. J Heat and Mass Transfer*, Vol. 33, pp. 1331-1338.
- Siegel, Robert, and Howell, John, 2002, *Thermal Radiation Heat Transfer*, 4th edition.
- Stone, H. L., 1968, Iterative Solution of Implicit Approximations of Multidimensional Partial Equations, *SIAM J. Numer. Anal.* vol 5, pp. 530-558.
- Yanenko, N. N. (1971). *The method of fractional time steps: the solution of problems of mathematical physics in several variables*, M . Holt (Editor), Springer-Verlag, New York.
- Trimis, D., and Durst, F., 1996, Combustion in a Porous Medium *Advances and Applications*, *Combust. Sci. Technol*, Vol. 121, pp. 153-168.

8. RESPONSIBILITY NOTICE

The author is the only responsible for the printed material included in this paper.